

Rapid Communications

Rapid Communications are intended for the accelerated publication of important new results and are therefore given priority treatment both in the editorial office and in production. A Rapid Communication in Physical Review B should be no longer than four printed pages and must be accompanied by an abstract. Page proofs are sent to authors.

X-ray-absorption fine structure in embedded atoms

J. J. Rehr

Department of Physics, University of Washington, Seattle, Washington 98195

C. H. Booth and F. Bridges

Department of Physics, University of California Santa Cruz, Santa Cruz, California 95064

S. I. Zabinsky

Department of Physics, University of Washington, Seattle, Washington 98195

(Received 2 December 1993)

Oscillatory structure is found in the atomic background absorption in x-ray-absorption fine-structure (XAFS) measurements. This atomic XAFS (AXAFS) arises from scattering within an embedded atom, and is analogous to the Ramsauer-Townsend effect. Calculations and measurements confirm the existence of AXAFS and show that it can dominate contributions such as multielectron excitations. The structure is sensitive to chemical effects and thus provides a probe of bonding and exchange effects on the scattering potential.

The main features of x-ray absorption spectra $\mu(E)$ are due to one-electron transitions from deep core levels. In molecules and solids, oscillatory fine structure exists in $\mu(E)$ due to scattering of the photoelectron by neighboring atoms. The well known technique of x-ray-absorption fine-structure (XAFS) measurements, which includes both extended-XAFS and x-ray-absorption near-edge structure (XANES), is based on the analysis of this fine structure. In XAFS the oscillatory part χ is defined relative to an assumed smooth "atomic-background" absorption $\mu_0(E)$, i.e., $\chi = (\mu - \mu_0)/\mu_0$. A complication is that $\mu_0(E)$ is not necessarily smooth. For example, the background may exhibit such well known structures as white lines, resonances, and jumps due to multielectron transitions, even well above threshold. Less well known, however, is the possible fine structure in $\mu_0(E)$ itself, in molecules and condensed systems, as discussed by Holland *et al.*¹ The purpose of this study is to show that this atomic x-ray-absorption fine structure (AXAFS) can produce large oscillations, has an XAFS like interpretation, and can alter XAFS analysis. In view of recent advances in XAFS theory and analysis techniques,²⁻⁴ in which the background plays a crucial role, this structure is now particularly important.

This extra fine structure originates from resonant scattering "in the periphery of the absorbing atom."¹ The effect is like an internal Ramsauer-Townsend (RT) resonance where the incident electron is a spherical wave created at the center of the atom, rather than a wave scattered by an atom. As the photoelectron electron approaches a potential barrier—in this case the edge of an

embedded atom potential—the reflection coefficient oscillates with energy, with a pronounced increase just above threshold, followed by a dip and subsequent oscillations that conserve integrated oscillator strength. We find that AXAFS can be the dominant background fine structure and has features in the same energy range as multielectron transitions, complicating detection of the latter. Using a recent background-subtraction technique,³ experimental backgrounds for Ba, Ce, and Pr *K* edges are obtained which exhibit AXAFS as large as 60% of the XAFS amplitude. Theoretical calculations² based on an *ab initio* XAFS and/or XANES code FEFF 5X confirm these observations. To our knowledge, the only previous attempt¹ to identify AXAFS was only partly successful, and the work did not derive its oscillatory character. Also, notable discrepancies between theory and experiment were found at low energies, and no attempt was made to observe AXAFS in crystalline solids. We believe, however, that evidence for AXAFS exists in many previous studies, although not heretofore identified as such. In particular we suggest that AXAFS is largely responsible for the spurious peak at about half the first neighbor distance often observed in XAFS Fourier transforms.^{3,5}

XAFS analysis differs from low-energy electron diffraction and other spectroscopies where the full theoretical spectrum is compared with experiment. Although the XAFS spectrum $\chi(E)$ can now be calculated remarkably well (< 1% errors for many systems), some features in background absorption spectra $\mu_0(E)$ in solids are not yet as well described by theory. Deviations typically about 5% have been found in the few cases where de-

tailed comparisons have been made, and systematic errors in absorption measurements are a further complication. Consequently, theoretical background functions are not usually used to fit the full absorption spectra $\mu(E)$.

Until recently, estimating the background by a smooth spline through the XAFS has been the standard approach in detailed XAFS analyses. However, a number of improved background subtraction techniques have recently been developed.^{3,4} The approach adopted here³ is based on an iterative procedure, which makes use of the high quality of present theoretical XAFS functions. After removing the pre-edge absorption, a smooth spline function is fit to the absorption data $\mu(E)$ (Fig. 1), which simulates to lowest order the free atomic absorption $\mu_0(E)$ without XAFS or other features present. Then a trial XAFS function $\chi(E) = [\mu(E)/\mu_0(E)] - 1$ is obtained. A Fourier transform of χ with respect to wave number k defined with respect to threshold energy E_0 , yields peaks in r space corresponding to the distribution of neighbors to the absorbing atom. Initially, the transforms often have a spurious, r space peak near 1 Å that is inconsistent with their known structures. Next an approximate fit of the first few peaks of the r space transform is made using theoretical XAFS standards.⁶ This fit is transferred back to energy space and subtracted from the experimental data to remove most of the low-frequency XAFS oscillations. A high-order spline is used to smooth the remaining data (Fig. 1). The positions of the knots in this spline are varied to follow the larger features in the residue. This spline function then becomes a different

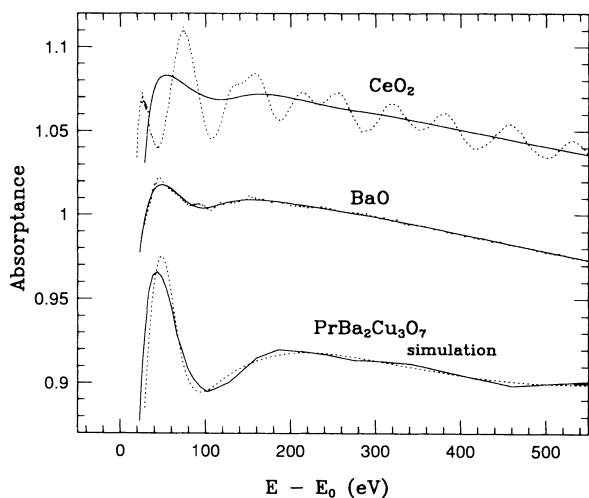


FIG. 1. Top curves: Ce K -edge absorption $\mu(E)$ (dotted) and $\mu_0(E)$ (solid) from CeO_2 vs energy E above the Ce K edge (40 441 eV). All spectra in this paper have their step height normalized to unity, and shifted as displayed. The oscillatory structure above the edge (dotted) is the XAFS. The solid curve is the experimentally obtained “atomic background” absorption $\mu_0(E)$ (see text). Note the sharp dip in this background at ≈ 115 eV. Middle curves: residue function and fit for Ba K -edge data from BaO. The residue functions are the difference between the data and the fit in E space, i.e., $\mu_{\text{res}}(E) = \mu(E)/[\chi_{\text{fit}}(E) + 1]$. Bottom curves: simulated background (solid) and extracted background (dotted) as a test of our extraction method.

$\mu_0(E)$ and an XAFS function is extracted. The process is iterated to convergence, typically in several iterations. With this procedure the background $\mu_0(E)$ contains all the atomic fine structure and the spurious r space peak near 1 Å is eliminated.

This procedure was tested on a theoretical absorption spectrum from FEFF 5X for a model of $\text{PrBa}_2\text{Cu}_3\text{O}_7$ (PBCO) which included many XAFS shells and a background with the above RT-like resonance. PBCO was chosen because the contribution from higher shells is significant. This check therefore tests both the fit to the XAFS and to the background. The extracted background fits the simulated background well (Fig. 1).

This procedure was then applied to Ba, Ce, and Pr K -edge data of BaO, CeO_2 , and PBCO. The data were collected at $T \approx 80$ K, at the Stanford Synchrotron Radiation Laboratory (SSRL) using (400) monochromator crystals on beam line 10-2. Details are given in a separate paper.⁷ The extracted backgrounds of all these high energy K edges (Fig. 2) are similar in shape and energy scale, exhibiting the near-edge peak and dip structure

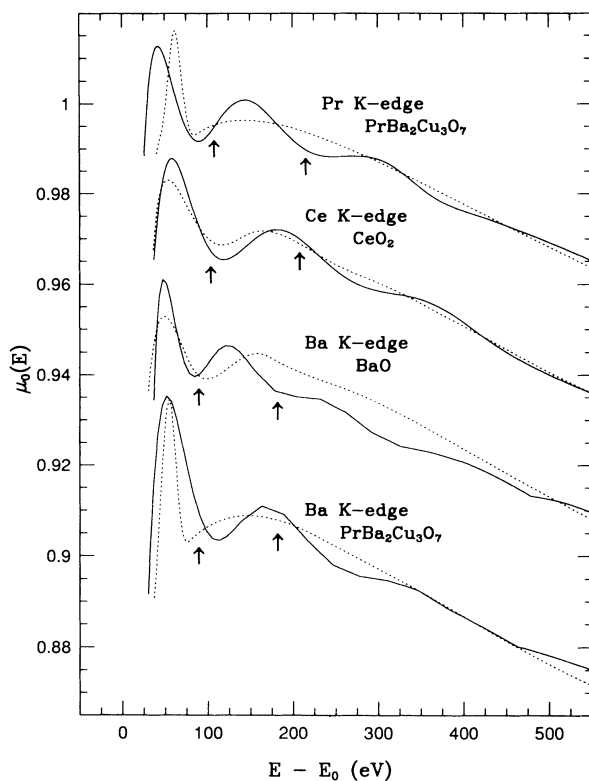


FIG. 2. Experimental (dotted lines) and theoretical (solid lines) background absorptions, $\mu_0(E)$, for the Ba, Ce, and Pr K edges of BaO, CeO_2 , and PBCO. ΔE is the energy above threshold, i.e., 37 444 40 441, and 41 991 eV for the Ba, Ce, and Pr edges, respectively. Both the experimental and the theoretical backgrounds have been adjusted to fit the Victoreen formula with a fourth-order polynomial. The calculations are currently limited by discontinuities at R_{mt} which can effect the AXAFS amplitude. The BaO calculation has an additional threshold energy shift of +20 eV. Arrows indicate the positions of $Z + 1$ excitation thresholds.

consistent with that expected for a RT resonance. The magnitude of this structure is comparable to EXAFS amplitudes and is a factor of four larger than the step-like structures observed above the edge for the rare gas Kr or for the Rb and Br K -edge data for RbBr.

We now briefly discuss the theory of AXAFS and show that it has an interpretation analogous to the curved-wave theory of XAFS.⁸ "Embedded atoms" in solids may be defined in terms of their respective scattering potentials. The final-state potential v_0 at the absorption site consists of a bare atomic potential v_a , plus extra-atomic contributions v_e from the tails of the electron distributions of neighboring atoms. In the muffin-tin approximation,

$$\begin{aligned} v_0(r) &= v_a(r) + v_e(r) \quad (r < R_{\text{mt}}), \\ &= v_{\text{mt}}, \quad (r \geq R_{\text{mt}}), \end{aligned} \quad (1)$$

where R_{mt} is the muffin-tin radius. For simplicity we consider a one-electron calculation of photoabsorption by an embedded-atom using the Fermi "golden rule" and the dipole approximation, i.e.,

$$\mu_0(E) = 4\pi^2\alpha\omega \sum_f |\langle c|\hat{\epsilon} \cdot \vec{r}|f\rangle|^2 \delta(E - E_f), \quad (2)$$

where $\alpha \simeq 1/137$ is the fine-structure constant, ω is the x-ray energy (we use Hartree atomic units $e = m = \hbar = 1$), $E = \omega - E_c$ is the photoelectron energy, $\hat{\epsilon}$ is the x-ray polarization vector, and the final states $|f\rangle = (1/r)R_0(r)Y_{lm}(\hat{r})$ are calculated at energy $E_f = (1/2)k^2$ in the embedded-atom potential v_0 . The normalized radial wave functions $R_0(r)$ are obtained by matching the regular solution of the radial l -wave Schrödinger equation to the asymptotic form $R_0(r) = kr[j_l(kr) \cos \delta_l - n_l(kr) \sin \delta_l]$, $r \geq R_{\text{mt}}$, where j_l and n_l are spherical Bessel functions, δ_l is the l th partial wave's phase shift, and l is fixed by dipole selection rules. This matching procedure is equivalent to a calculation of the Jost function $F_l(E)$ which guarantees final state normalization, as discussed by Holland *et al.*¹ and by Newton.⁹ In particular Holland *et al.* show that the atomic cross section can be written as $\mu_0/|F_l|^2$, where $\tilde{\mu}_0$ is a reduced matrix element which varies smoothly with energy. All of the calculations of AXAFS reported here are based on an analogous matching procedure for the relativistic spinor wave functions used in FEFF, without any of the simplifying approximations of the following discussion. Additional details will be given elsewhere.¹⁰

The formal relations⁹ satisfied by the Jost function are very general and do not explicitly show the oscillatory behavior of AXAFS. Thus to illustrate its nature we present a highly simplified model based on first-order perturbation theory with respect to the free atom potential. We will assume that the free atomic background has negligible oscillatory structure; sample calculations with large muffin-tin radii support this assumption. Using the spectral representation of the embedded-atom Green's function, the final-state sum in Eq. (2) can be expressed as $\sum_f |f\rangle \delta(E - E_f) \langle f| = (-1/\pi) \text{Im} G_0$ where $G_0 = (E - H_0 + i0^+)^{-1}$ is the embedded-atom Green's function (operator) and H_0 the embedded-atom Hamiltonian. To

first order in the perturbation $\delta v = v_0(r) - v_a(r)$, G_0 is given by $G_0 \simeq G_a + G_a \delta v G_a$, where G_a is the free atomic Green's function. For deep core absorption, the core states are highly localized so we need only evaluate G_0 in position space for very small arguments r and r' , where δv is negligible. The radial part of G_a ,⁹ is given by $G_a(r, r') = (-1/k)R_a(r<)R_a^+(r>)$, where $r_{>(<)}$ is the greater(lesser) of r and r' , and $R_a^+ = S_a + iR_a$ is the outgoing part of the radial Schrödinger equation. Combining these ingredients, one finds that $\mu(E)$ can be factored as in conventional XAFS theory,¹¹ i.e., $\mu_0 = \mu_a(1 + \chi_e)$, where μ_a is given by Eq. (2) calculated with free atomic states $|f_a\rangle$ and the AXAFS χ_e is

$$\chi_e \simeq -\text{Im} \frac{1}{k} \int_0^\infty dr [R_a^+(kr)]^2 \delta v(r). \quad (3)$$

An analogy to the curved-wave XAFS formula⁸ is obtained by recognizing that the perturbation arises from the periphery of the atom where one may approximate R_a^+ by its asymptotic form, $R_a^+ \simeq c_l(kr) \exp(ikr + i\delta_l^a)$. Here $c_l(kr)$ is the curved wave factor⁸ in the spherical Hankel function $h^{(+)}(kr) = c_l(kr) \exp(ikr)/kr$. For simplicity we model the perturbation as $\delta v(r) \simeq v_{\text{mt}}/\{1 + \exp[\zeta(R_{\text{mt}} - r)]\}$, where ζ characterizes the decay of the atomic potential tails near R_{mt} . The integral (3) can then be expressed as

$$\chi_e = -\frac{1}{kR_{\text{mt}}^2} |f_e| \sin(2kR_{\text{mt}} + 2\delta_l^a + \Phi_e), \quad (4)$$

where $f_e = |f_e| \exp(i\Phi_e)$ is an effective curved-wave scattering amplitude. With the above model the AXAFS is analogous to a damped harmonic oscillator, $f_e \sim \exp(-2\pi k/\zeta)/k$. For comparison to experiment, Eq. (4) should have a few additional factors as in the usual XAFS formula, namely an amplitude reduction factor S_0^2 , a Debye-Waller factor, $\exp[-2\sigma^2(R_{\text{mt}}/R)^2 k^2]$, and a mean-free path term, $\exp(-2R_{\text{mt}}/\lambda)$.

AXAFS comparisons between the theoretical calculations and experimental results presented here are in reasonable agreement with each other (Fig. 2), especially for the simple oxides. The discrepancy at the edge for BaO is not fully understood, but may point to errors in FEFF's muffin-tin potential and energy reference. The long-range oscillatory structure in the calculations is likely due to a small discontinuity in FEFF's muffin-tin potential at R_{mt} .

To check whether multielectron excitations might also be present, we used the $Z + 1$ model to estimate where the step for a two-electron excitation would begin. In this model excitation energies correspond to the ionization energies of $Z + 1$ atoms, and are 99 eV for Ba and 113 eV for Ce, as indicated by arrows in Fig. 2. Small features in the background were previously attributed to multielectron excitations based on this model.^{3,4} However, it is likely that part of the observed structure can also be attributed to AXAFS.

We point out that our calculations of the atomic backgrounds shown in Fig. 2 were all done with ground-state exchange potentials. We found that the usual Hedin-

Lundqvist self-energy model used in FEFF (Ref. 6) gives too large an oscillatory amplitude near threshold. This is an indication of the sensitivity of the AXAFS to the exchange interaction. Evidently improvements to FEFF's muffin-tin potentials are necessary, and AXAFS may be useful in assessing various improvements.

It is well known that simple, monotonic approximations to the atomic background are not sufficient to obtain accurate XAFS data, emphasizing the importance of improved background removal methods.^{3,4} However, the atomic background μ_0 and the XAFS χ are tightly linked by the definition $\chi = (\mu - \mu_0)/\mu_0$, so the backgrounds obtained for theoretical and experimental standards may differ. Thus an understanding of AXAFS is essential to obtain experimental backgrounds. This difference also affects XAFS analysis; if one tries to isolate a Ce-O standard without taking its oscillatory background into account, one cannot obtain a good fit to the first Pr-O peak in PBCO. The inclusion of extra-atomic contributions in the atomic background may at first seem arbitrary. For example, the XAFS could be defined with respect to the bare atomic background, which is independent of the environment. However such a definition is problematical and inconsistent with multiple scattering theory based on independent scattering sites; also because the exchange interaction is not additive, it is not possible to construct the scattering potential by superposing free atomic potentials.

For the materials discussed in this paper, the

AXAFS is quite large, and is the dominant contribution to the background fine structure, exceeding multielectron effects in magnitude. *Ab initio* calculations of the AXAFS agree reasonably well with these observations and with the simplified model introduced here. The size and character of these background features, particularly their interference with the first coordination shell peak, indicate that accurate fits to XAFS data must take them into account. AXAFS is also interesting in its own right, because it depends critically on the scattering potential in the outer part of the absorbing atom. Thus, it provides a new and useful probe of chemical effects, the electron self-energy, core-hole effects, and other contributions to the embedded-atom potentials.

We thank J. B. Boyce, G. G. Li, P. Līviņš, M. Newville, B. Ravel, E. A. Stern, and Y. Yacoby for comments and discussions concerning background removal methods and T. Claeson for assistance in collecting the data. One of us (J.J.R.) also thanks the Institut für Experimentalphysik of the Freie Universität Berlin for hospitality, where part of this work was completed. SSRL is operated by the U.S. Department of Energy, Division of Chemical Sciences, and by the NIH, Biomedical Resource Technology Program, Division of Research Resources. The data were collected under UC/National Labs PRT time. This work was supported in part by U.S. DOE Grant No. DE-FG06-ER45415 (J.J.R. and S.I.Z.), and by NSF Grant No. DMR-92-05204 (C.H.B. and F.B.).

¹ B. W. Holland, J. B. Pendry, R. F. Pettifer, and J. Bordas, *J. Phys. C* **11**, 633 (1978).

² J. J. Rehr, *Jpn. J. Appl. Phys.* **32**, 8 (1993).

³ G. G. Li, F. Bridges, and G. S. Brown, *Phys. Rev. Lett.* **68**, 1609 (1992).

⁴ M. Newville, P. Līviņš, Y. Yacoby, J. J. Rehr, and E. A. Stern, *Phys. Rev. B* **47**, 14126 (1993).

⁵ A. I. Frenkel, E. A. Stern, M. Qian, and M. Newville, *Phys. Rev. B* **48**, 12449 (1993).

⁶ J. J. Rehr, R. C. Albers, and S. I. Zabinsky, *Phys. Rev. Lett.* **69**, 3397 (1992); J. J. Rehr, J. Mustre de Leon, S. I.

Zabinsky, and R. C. Albers, *J. Am. Chem. Soc.* **113**, 5135 (1991).

⁷ C. H. Booth, F. Bridges, J. B. Boyce, T. Claeson, Z. X. Zhao, and P. Cervantes, *Phys. Rev. B* **49**, 3432 (1994).

⁸ J. J. Rehr and R. C. Albers, *Phys. Rev. B* **41**, 8139 (1990).

⁹ R. G. Newton, *Scattering Theory of Waves and Particles*, 2nd ed. (Springer, New York, 1982).

¹⁰ S. I. Zabinsky, A. Ankudinov, J. J. Rehr, and R. C. Albers (unpublished).

¹¹ P. A. Lee and J. B. Pendry, *Phys. Rev. B* **11**, 2795 (1975).